Desalination and Water Treatment
www.deswater.com

doi: 10.5004/dwt.2022.29111

280 (2022) 224–239
December

Enhanced removal of cefixime from aqueous solutions using Fe_3O_4@GO nanocomposite with ultrasonic: isotherm and kinetics study

Farzad Mahdavian[a,b], Abdollah Dargahi[c,d], Mehdi Vosoughi[b,c,*], Ahmad Mokhtari[b], Hadi Sadeghi[b], Yousef Rashtbari[a,b]

[a]*Students Research Committee, Ardabil University of Medical Sciences, Ardabil, Iran, email: u3f.rashtbari@gmail.com (Y. Rashtbari)*
[b]*Department of Environmental Health Engineering, School of Health, Ardabil University of Medical Sciences, Ardabil, Iran, Tel. +989120910243; email: mvn_20@yahoo.com (M. Vosoughi), Tel. +989143062539; email: s.a.mokhtari@gmail.com (A. Mokhtari), Tel. +989144527948; email: hsadeghi1079@gmail.com (H. Sadeghi)*
[c]*Department of Environmental Health, Khalkhal University of Medical Sciences, Khalkhal, Iran, Tel. +989141597607; email: a.dargahi29@yahoo.com (A. Dargahi)*
[d]*Social Determinants of Health Research Center, Ardabil University of Medical Sciences, Ardabil, Iran*

Received 15 July 2022; Accepted 4 November 2022

ABSTRACT

Antibiotics, including cefixime (CEX), are widely used in medicine and veterinary medicine and enter aquatic environments through various pathways such as agricultural runoff, direct discharge from municipal wastewater treatment plants, human excreta, direct disposal of medical, veterinary, and industrial wastewaters. The aim of this study was to investigate the applicability of GO (graphene oxide)-Fe_3O_4 nanocomposite with ultrasonic (US) in the removal of CEX from aqueous solutions. To conduct the experiments of this experimental-lab scale study, application of the response surface methodology was considered. The effect of important operational parameters such as solution pH, nanocomposite concentration, initial concentration of CEX, and reaction time was investigated at three levels (+1, 0, and –1) with a constant ultrasound intensity at 37 kHz. The optimization and analysis of the results were performed by Design-Expert 10 and Statgraphics software, and the residue of CEX was measured using a spectrophotometer at 288 nm. The results showed that the quadratic model was suitable for the data (P-value < 0.0001), and the proposed model (quadratic) was approved with a high correlation coefficient (R^2 = 0.9824 and $R^2_{Adj.}$ = 0.9670). Under the optimal conditions for the process (pH = 3, nanocomposite of 1 g/L, initial concentration of CEX of 10 mg/L, and reaction time of 90 min), the observed removal efficiency was about 100%. According to the results, the GO-Fe_3O_4/US process was approved to be effective in the degradation of the antibiotic CEX, and the Box–Behnken design was found to be a suitable tool to optimize the process conditions in the removal of CEX.

Keywords: Cefixime; Graphene oxide; Nanoparticles; Ultrasonic; Fe_3O_4; Box–Behnken; Adsorption

1. Introduction

In recent years, drug use and access to a variety of drugs have increased in the world due to the spread of disease and advances in medical and pharmacy science and therapeutic coverage [1–3]. The quality of available water resources is one of the challenges of communities around the world [4–6]. Antibiotics are widely used in the treatment or prevention of infectious diseases in medicine and veterinary medicine. Large quantities are also used in agriculture to improve fruit growth. Today, the use of drugs, especially antibiotics, is increasing. The production of

* Corresponding author.

drugs has been approximately 100,000–200,000 tons/y [7,8]. The rest of the antibiotics are excreted in the form of main compounds or metabolites as human or animal wastes and enter the wastewater network and wastewater treatment plant [9,10]. About 30%–90% of antibiotics are not metabolized in humans and animals and eventually enter the environment in the form of active compounds through urine and feces [11]. The discharge of antibiotics in wastewater treatment plants and secondary effluents from the antibiotic manufacturing industry is a very important source of their release into the environment [12]. Cefixime (CEX) is a broad-spectrum antibacterial that has the ability to fight a variety of pathogens, especially gram-negative organisms [13–15]. CEX is used to treat infections such as the upper and lower respiratory tract, middle ear, paranasal sinuses, urinary tract, and gonorrhea [16]. The decomposition of these compounds is considered as an important ecological challenge due to their complex structure and low biodegradability [17]. Methods used in this field include chemical oxidation [18], membrane processes [19], ionization [20], and adsorption [21]. Removal and bioremediation of antibiotics are difficult due to the presence of a stable ring of naphthol (as the main structure) and its toxicity to microorganisms. Also, since the ratio of biochemical oxygen demand (BOD) to chemical oxygen demand (COD) is small in many industrial effluents, the use of non-biological methods, especially chemical processes, is recommended [22,23]. The adsorption process, compared to other treatment techniques, has received more attention in terms of initial cost, wastewater reuse, simplicity and flexibility in design, easy operation, and insensitivity to contaminants and toxic compounds. The production of high-quality effluent and the absence of free radicals and hazardous substances are other advantages of this method [24,25].

Application of ultrasonic wave techniques, along with other methods such as the adsorption process, is the most common way to use ultrasonic waves. In this case, the use of ultrasonic waves accelerates the chemical process due to the phenomenon of acoustic cavities, that is, the formation and growth and immobility of micrometer-sized cavities caused by the propagation of waves through the liquid. Also, ultrasonic waves and their secondary effects are the growth and bursting of small gas bubbles that cause more mass transfer and cause fundamental changes between the adsorbate and the adsorbent without changing the equilibrium properties of the adsorbent–adsorbate [26].

Graphene, as a new allotropic type of carbon allotropes, can be a good solution to many environmental problems. Graphene nanosheets have a carbon layer where the atoms are placed in a two-dimensional honeycomb network. Such a structure of graphene has led to properties such as mechanical strength, larger surface area, and thermal and electrical conductivity [27]. In a graphene plate, each carbon atom has an off-plane orbital. This orbital is a good place to bond with functional groups as well as hydrogen atoms. The bond between the carbon atoms in the plane is covalent and very strong. Graphene oxide has oxygen groups such as (C=O–, –COOH, –O–, and OH); however, the separation of graphene oxide requires a lot of energy from aqueous solutions, which can be solved by adding magnetic nanoparticles to aqueous solutions. Among different magnetic materials, Fe_3O_4 is considered due to its corrosion resistance, magnetic structure, and easy and fast separation [28].

Experimental design is one of the low-cost, simple, and effective methods and the best tool to study the effect of process parameters of the process separately and their interaction with each other simultaneously [29,30]. One of the models used in experimental design is the response surface methodology, which is a simple, effective, low-cost method for optimizing various processes. Another advantage of this method is the ability to perform an analysis of variance to determine the final removal formula and determine the optimal theoretical conditions. This method can be done by the central composite design (CCD) method or the Box–Behnken design (BBD) [31,32]. The BBD method is a second-order design based on three-level factorial designs. This method can estimate the amount of parameters in a quadratic model and calculate the amount of non-compliant parameters by performing the required designs [33,34]. In this study, the surface response method (RSM) was used to design the BBD model for optimization and evaluation of the effect of independent variables on response performance (removal efficiency) and, on the other hand, for prediction of the best response value. In this study, ultrasonic (US) has been used to accelerate the chemical process by creating the phenomenon of cavitation. Some of the researchers have carried out the ultrasonic method to develop the advanced oxidation process (making OH radicals) for the degradation of pollutants. One of the most common methods of removing contaminants from aqueous media is to use the ultrasonic process along with other oxidizers. In the present study, we used ultrasonic to increase the efficiency of the adsorption process, not for AOP, which is a rarely studied hybrid method used for adsorbents.

In this study, ultrasonic has been used to accelerate the chemical process by creating the phenomenon of cavitation. Ultrasound, in addition to creating the cavitation phenomenon, increases the material transfer rate in the adsorption process. This combined method is a new method to increase the adsorption, and the innovation of this study was the use of graphene oxide magnetic nanomaterial along with the ultrasonic for acceleration of antibiotic adsorption process.

2. Materials and methods

2.1. Chemicals

In this study, CEX antibiotic with the chemical formula ($C_{16}H_{15}N_5O_7S_2$) and a molecular weight of 453.452 g/mol; the chemical structure of mentioned antibiotic is shown in Fig. 1 [17], and it was produced by Sigma-Aldrich Company and was used in the preparation of the stock solution. Also, H_2SO_4 and NaOH prepared by Merck Company, Germany (laboratory purity) were used to adjust the pH of the solution. Double distilled water was used in all stages of the experiments. X-ray diffraction for GO, Fe_3O_4 nanoparticles, and Fe_3O_4@GO nanocomposite in the angle range of $2\theta = 40.5$ was determined by X-ray diffraction (XRD) device in the laboratory of Bim Gostar Taban Company (Model: PW1730, Company: Philips, Country: Holland, Tube: Co, λ: 1.54056 Å, step size: 0.05°/s, voltage: 40 kV, and current: 40 mA), as shown in Fig. 2.

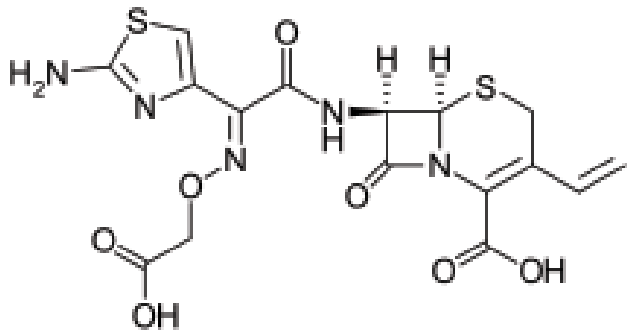

Fig. 1. Chemical structure of CEX.

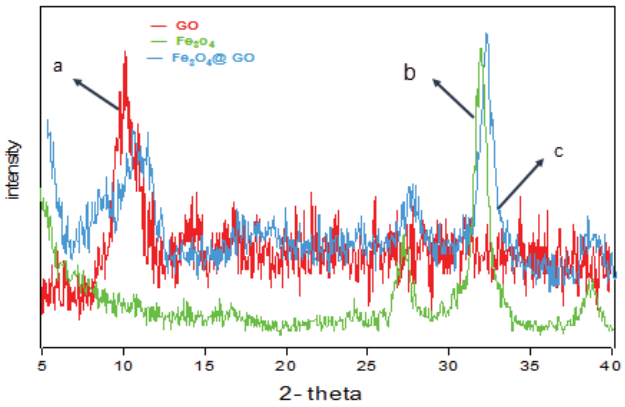

Fig. 2. (a) X-ray diffraction pattern of graphene oxide (GO), (b) nanoparticles (Fe_3O_4), and (c) nanocomposite (Fe_3O_4@GO).

2.2. Synthesis of Fe_3O_4 nanoparticles

Fe_3O_4 magnetite nanoparticles were synthesized by the chemical co-precipitation method. In this method, 5.4 g of $FeCl_3{\cdot}6H_2O$ and 2.87 g of $FeCl_2{\cdot}4H_2O$ (a weight ratio of two to one in 100 mL of ion-free water) were mixed in a round bottom balloon in an atmosphere of nitrogen gas. Then, 25% ammonia solution was added dropwise to the solution until the pH of the solution reached 9, and finally, a black precipitate containing magnetite nanoparticles was formed. The formed precipitate was stirred for 30 min and heated to 80°C, then washed three times with deionized water and twice with ethanol. All materials in this part were prepared by Merck Company, Germany [35].

2.3. Loading of Fe_3O_4 nanoparticles on graphene oxide

After preparing graphene oxide and synthesizing Fe_3O_4 nanoparticles, 1.25 g of Fe_3O_4 nanoparticles were poured into 200 cc of distilled water and placed on a magnetic stirrer for 10 min to homogenize the solution. Then, 3.75 g of graphene oxide was poured into the solution and placed on a magnetic stirrer for 2 h at a speed of 500 rpm to load Fe_3O_4 nanoparticles onto graphene oxide. The prepared nanocomposite was then separated with filter paper, washed several times with distilled water twice, and then placed in an oven at 95°C to dry [36].

2.4. Characterization of pilot and equipment used

This experimental study was performed on a laboratory scale with intermittent flow. 0.1 M was used to adjust the pH of the solution with sulfuric acid and sodium hydroxide. Different concentrations of CEX (mg/L) were used by the stock solution. At the end of the reaction time, the solution was sampled and centrifuged at 3,000 rpm and then filtered using a 0.22-micron filter to ensure the separation of the nanocomposite. The concentration of residual CEX was measured using a DR5000 spectrophotometer (HACH) at 288 nm [37]. Finally, the removal efficiency of CEX was calculated using Eq. (1) [38].

$$\%\text{Removal} = \frac{C_0 - C_t}{C_0} \times 100 \quad (1)$$

where C_0: Initial concentration of CEX (mg/L); C_t: CEX concentration after reaction (mg/L).

2.5. Experimental design and statistical analysis

In this study, the surface-response method based on the BBD was used to optimize and determine the effect of parameters and simultaneous interaction between variables on the response (removal of CEX) using Design-Expert Software version 10. The studied variables include pH, contact time, nanocomposite dosage, and initial concentration of CEX. In this study, the BBD method at three levels (+1, 0, –1) combined with the RSM method was used to design the experiment and optimize the process. The number of experiments required was determined by the response level method using the BBD model based on the equation of $N = 2^K (K–1) + C$. In the mentioned equation, N is the number of test samples, K is the number of variables, and C is the number of center points [39]. The observed CEX removal efficiency was considered as a dependent variable (response). The four studied factors, along with the selected levels and range, are presented in Table 1. The number of experiments obtained through design by the BBD method was 31. To ensure the reproducibility of the experiments, all experiments were performed with three replications (criterion: RSD < 0.05). Central points were selected as a method for estimating and evaluating experimental error and measuring the lack-of-fit. The statistical significance of quadratic fit models was determined using the lack-of-fit test (LOF), correlation coefficient, and adjusted correlation coefficient between laboratory and predicted values (R^2, $R^2_{\text{Adj.}}$).

3. Results and discussion

3.1. Characterization of nanocomposite

3.1.1. XRD analysis

X-ray diffraction for GO, Fe_3O_4 nanoparticles, and Fe_3O_4@GO nanocomposite in the angle range 2θ = 10°–40° was determined by XRD (Model: PW1730, Philips). In the GO model, the peaks generated at an angle of 11.4° are related to functional groups, including oxygen. This reflection confirms the structure of graphene along with

Table 1
Experimental design levels of chosen variables

			Levels		
Variable	Sign	Unit	–1	0	+1
Initial pH of solution	*A*	–	3	7	11
Nanocomposite concentration	*B*	g/L	0.2	0.6	1
Contact time	*C*	min	10	50	90
Initial concentration of CEX	*D*	mg/L	10	30	50

oxygenated functional groups and indicates strong oxidation of graphite and proper synthesis of graphene oxide. In the Fe_3O_4, X-ray diffraction pattern, peaks formed at angles of 30.8° and 35.7° show the presence of iron oxide particles in the structure of Fe_3O_4 nanoparticles. A combination of peaks in the GO adsorbent and Fe_3O_4 nanoparticles in the Fe_3O_4@GO nanocomposite has been observed at these angles; thus, this analysis shows that iron particles have been successfully synthesized and deposited on carbon.

3.1.2. Fourier-transform infrared spectroscopy analysis

Fourier-transform infrared spectroscopy (FTIR) is based on the absorption of radiation and the study of vibrational mutations of multiatomic molecules and ions. This method is used to determine the structure, measure chemical species, and identify organic compounds. The results of the spectrum in the range of 450–4,000 cm^{-1} were prepared by Perkin Elmer (model: Two Spectrum). Fig. 3 shows the FTIR analysis to determine the functional groups present on the Fe_3O_4@GO nanocomposite surface. As can be seen in Fig. 3, in the GO pattern, the wavelengths are 3,416.33 and 1,591.88 cm^{-1} and correspond to the stretching vibrations of –OH and C=C, and the band of 1,039 cm^{-1} corresponds to the stretching vibrations of C–O. The peak of 578.08 cm^{-1} is related to Fe–O vibrational vibrations and the peak of 1637.4 cm^{-1} indicates the stretching band of C=O.

3.1.3. Scanning electron microscopy analysis

Scanning electron microscope (SEM model) (MIRA III TESCAN) was used to determine the surface and morphological characteristics of GO, Fe_3O_4 and Fe_3O_4@GO nanocomposite. SEM images of the nanocomposite are shown in Fig. 4 to clarify the morphological levels of GO, Fe_3O_4, and Fe_3O_4@GO. Fig. 4a contains a large amount of microporosity and shows very small pores on the adsorbent surface. Fig. 4b shows that Fe_3O_4 nanoparticles have a regular morphology and are uniform, homogeneous, and spherical. The particle size distribution was determined to be approximately 50 nm in size. Fig. 4c shows that a number of Fe_3O_4 nanoparticles tend to combine with GO, and a strong cluster-like accumulation is evident among them. The white particles observed in Fig. 4c on graphene oxide indicate the presence of Fe_3O_4 on the surface of this nanocomposite. The rough and uneven surface of Fe_3O_4 increases GO uptake sites [40,41].

Fig. 5 shows the magnetic curve of the Fe_3O_4 nanoparticles and the Fe_3O_4@GO nanocomposite. It can be seen that both adsorbents are magnetic at room temperature. The magnetic saturation of Fe_3O_4 nanoparticles and Fe_3O_4@GO nanocomposite is 57.18 and 8, respectively. As expected, the amount of magnetic saturation of the Fe_3O_4@GO nanocomposite was lower than that of Fe_3O_4 nanoparticles, which indicates the presence of GO in the nanocomposite, reducing the magnetic saturation. However, as the amount of magnetic saturation of the Fe_3O_4@GO nanocomposite decreases, it can still be attracted to the magnet, indicating a respectable magnetic response. The magnetic saturation of the Fe_3O_4@GO nanocomposite for rapid separation was

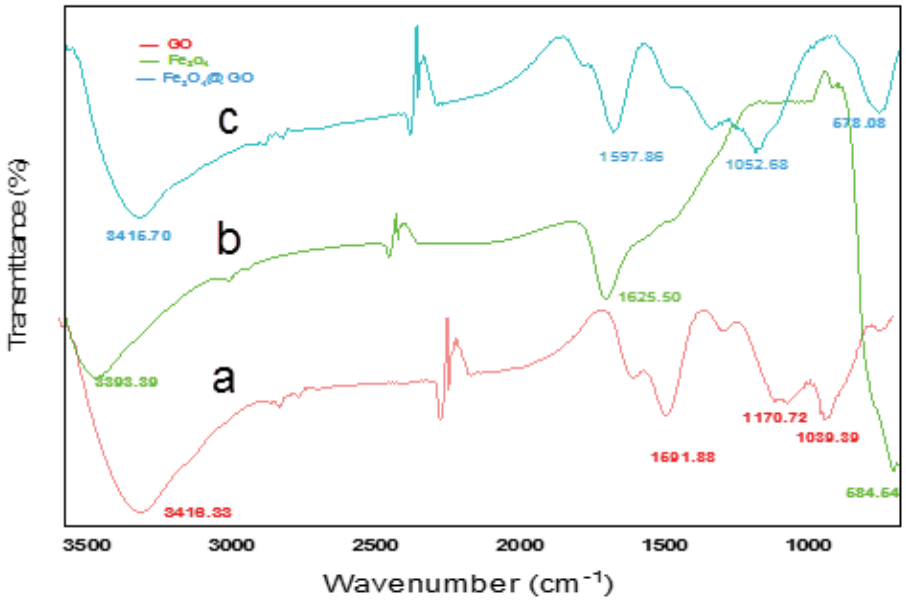

Fig. 3. FTIR spectroscopy of Fe_3O_4@GO nanocomposite.

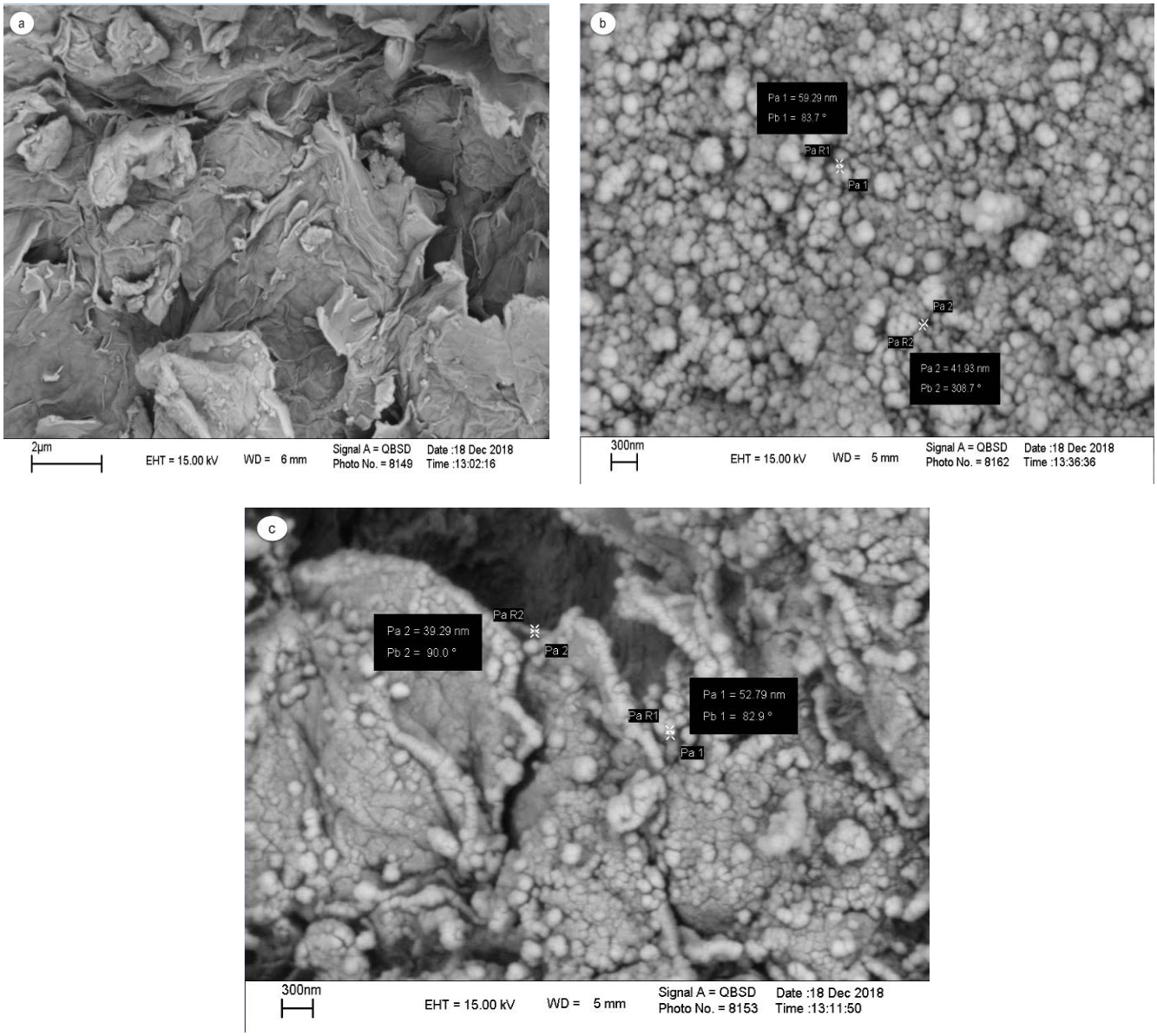

Fig. 4. Scanning electron microscope of GO (a), iron oxide nanoparticles (b) and Fe_3O_4@GO (c) composite images.

similar to previous studies. Therefore, it can be said that the nanocomposite synthesized in this study had a perfect magnetic property to be separated by a magnet.

3.2. Box–Benken statistical analysis

Choosing a suitable model for the system that can predict the results with high and appropriate accuracy is important and is the first step in analyzing the results. For this purpose, the proposed quadratic model was used. The proposed model for this system includes 4 terms of single effects (*A*, *B*, *C*, and *D*), six terms of interaction effects (*AB*, *AC*, *AD*, *BC*, *BD*, and *CD*), and four terms related to quadratic effects (A^2, B^2, C^2, and D^2). The *P*-value of analysis of variance (ANOVA) analysis was used to evaluate the model and test its significance. ANOVA results related to the removal of CEX are shown in Table 2. Based on the data in this table, the *P*-value for the proposed model is observed to be less than 0.0001. According to the remaining parameters in the system, the model is presented as Eq. (2) to predict the removal efficiency of CEX. This model is a set of single, interaction, and quadratic effects.

$$Y = +46.29 - 18.35A + 11.26B - 11.68C + 10.17D - 8.60AB + 4.06AC - 0.5625AD + 7.06BC + 11.16BD + 3.33CD + 8.78A^2 - 0.7937B^2 + 10.43C^2 - 12.29D \quad (2)$$

where *Y* is the predicted CEX removal efficiency in percentage, *A* is pH, *B* is the amount of nanocomposite (g/L), *C* is Time (min), and *D* is the initial concentration of CEX (mg/L).

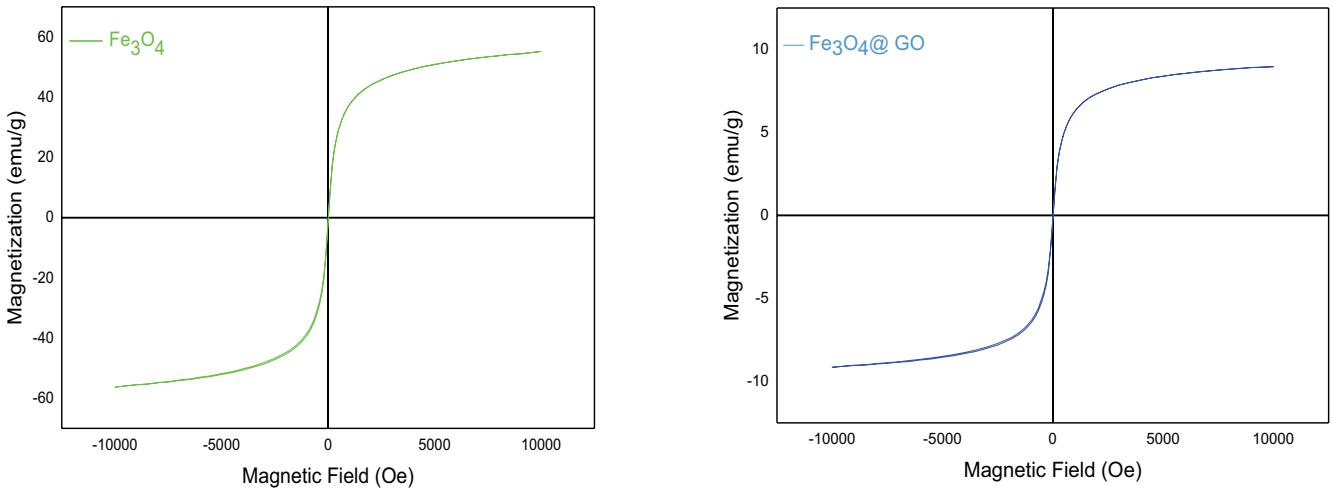

Fig. 5. VSM analysis for Fe_3O_4 nanoparticles and Fe_3O_4@GO nanocomposite.

Table 2
Analysis of variance of operational parameters in the removal of CEX from aqueous solutions using GO-Fe_3O_4/US

Source	Sum of source	Df	Mean square	*F*-value	*P*-value	Status
Model	12,218.13	14	872.72	63.80	< 0.0001	Significant
A-pH	4,038.84	1	4,038.84	295.27	< 0.0001	
B-Dose	1,521.68	1	1,521.68	111.25	< 0.0001	
C-Conc.	1,636.60	1	1,636.60	119.65	< 0.0001	
D-Time	1,239.93	1	1,239.93	90.65	< 0.0001	
AB	296.01	1	296.01	21.64	0.0003	
AC	65.85	1	65.85	4.81	0.0433	
AD	1.27	1	1.27	0.0925	0.7649	
BC	199.09	1	199.09	14.56	0.0015	
BD	498.63	1	498.63	36.45	< 0.0001	
CD	44.42	1	44.42	3.25	0.0904	
A^2	551.26	1	551.26	40.30	< 0.0001	
B^2	4.50	1	4.50	0.3293	0.5741	
C^2	777.70	1	777.70	56.86	< 0.0001	
D^2	1,079.37	1	1,079.37	78.91	< 0.0001	
Residual	218.85	16	13.68			
Lack of fit	174.75	10	17.48	2.38	0.1506	Not significant
Pure error	44.10	6	7.35			
Cor. total	12,436.99	30				
			(Correlation coefficient)			
R^2 = 0.9824			$R^2_{Adj.}$ = 0.9670		R^2_{Pred} = 0.9142	CV(%) = 7.60

The quality of the proposed model was evaluated using the values of correlation coefficient (R^2), adjusted correlation coefficient ($R^2_{Adj.}$), and predicted correlation coefficient (Pred. R^2) (the values of R^2 and $R^2_{Adj.}$ of the model were 0.9824 and 0.9670, respectively). The proximity of the two R^2 values and their slight differences indicate the acceptable accuracy of the proposed model and show a very good correlation between the results obtained by the experimental method and the predicted values by thestatistical method.

Fig. 6a shows the overlap of the predicted values against the observed values, as well as the amount of standardized residues for each run performed in Fig. 6b. According to the above diagrams, it can be concluded that for all experiments performed, the values of the standardized residues are in the acceptable range. Also, in Fig. 6c, the internally studentized residual values indicate the acceptance of the model in providing opportunities for analysis of variance.

Fig. 7 shows the effective variables considered for CEX removal (including pH, nanocomposite concentration, reaction time, and initial concentration of CEX), and determined optimal points.

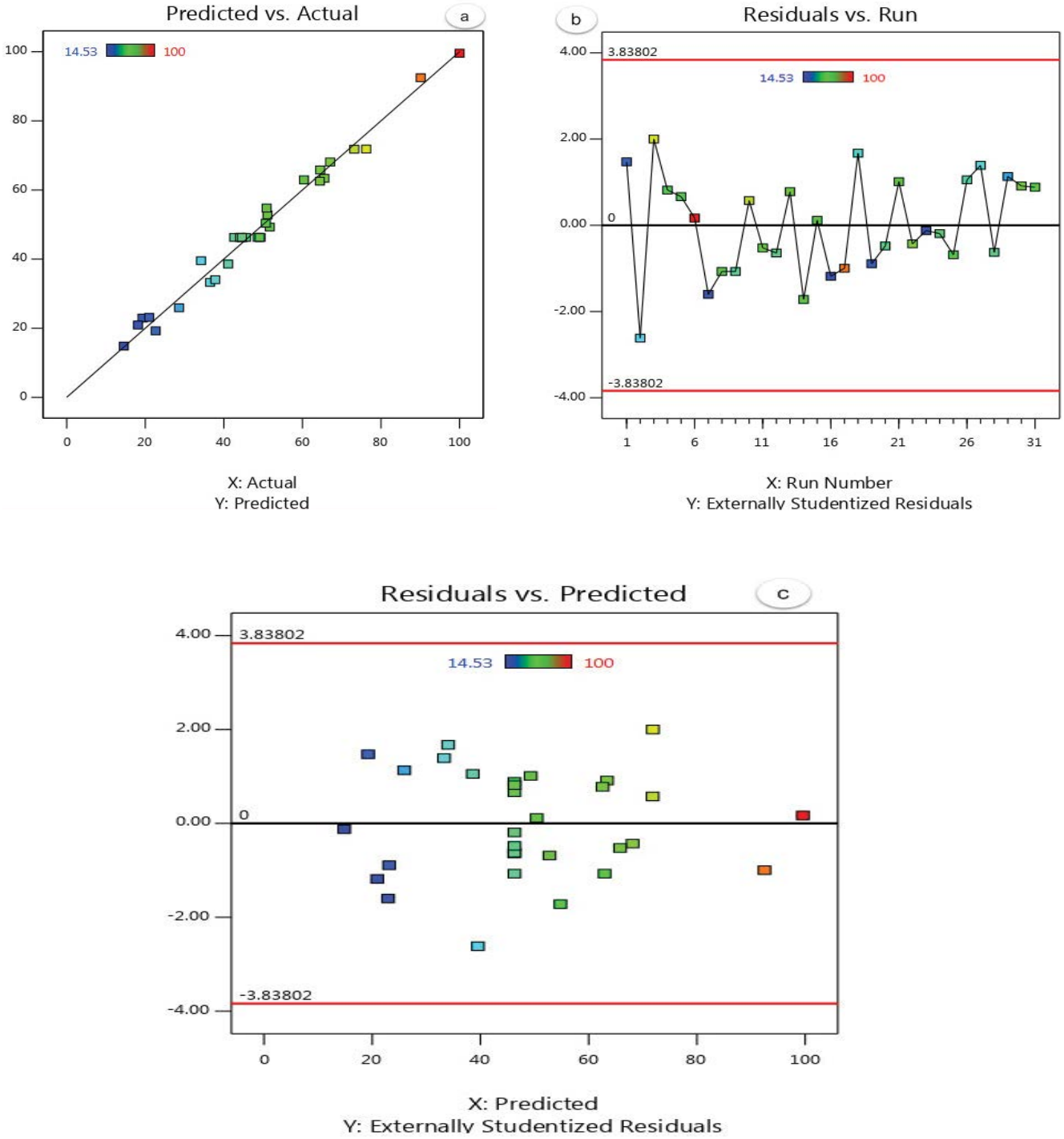

Fig. 6. Drawing the distribution of the tested data vs. the values predicted by the model.

In this study, the influence of factors affecting the removal process was also investigated by standardized Pareto diagrams. As shown in Fig. 8, the order of effect levels of parameters from high to low was as follows: pH > time > initial concentration > nanocomposite dose. In the study of Kamani et al. [42], the efficiency of the sonon-ocatalytic process was investigated using titanium dioxide nanoparticles for the removal of the erythromycin and metronidazole antibiotics from aqueous solution by the response surface methodology. In this study, considering the results of fitting different models on the data obtained in COD removal, the quadratic model had a higher fit, and the pH of the solution with $p < 0.0001$ is one of the most influential parameters.

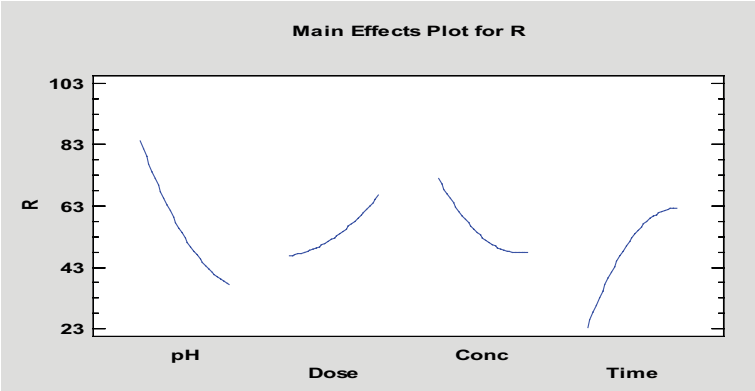

Fig. 7. Effect of the considered initial parameters (pH, dose (mg/g), concentration (mg/L), and time (min)) and their optimal points.

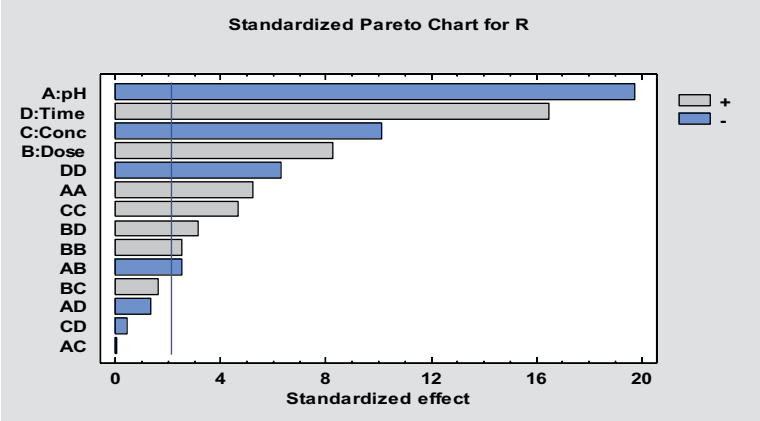

Fig. 8. Pareto chart for investigation of the extent and effect of factors on removal efficiency (*R*).

3.3. Effect of effective parameters in the removal of CEX

One of the advantages of graphene oxide is its easy dispersion in aqueous solution, which forms a stable colloidal dispersion. The functional groups around the graphene oxide plates are converted to carboxylic anions. Graphene oxide maintains its negative surface charge in the low pH range. This substance can easily be obtained from natural sources of graphene in nature. On the other hand, because graphene oxide has a high surface area, many scientists are looking to use it to remove contaminants from water. However, collecting graphene oxide from the water after the adsorption process is a problem that uses a magnetic composite to solve this problem.

3.3.1. Effect of pH

Fig. 9a shows the removal efficiency of CEX as a function of pH. The highest removal rate occurred at a pH of 3, and with increasing pH, a sharp decrease in removal rate was observed. pH is one of the most important parameters affecting removal efficiency. Previous studies have shown that pH plays an important role in the decomposition and removal of antibiotics [18–43]. As shown in Fig. 9a, there is a significant difference between the removal of CEX at different pH values, and the rate of degradation is significantly higher at acidic pH. The pH affects the adsorption capacity, dissociation of the target compounds, and the electrostatic charge distribution on the surface of the adsorbent. One of the reasons for increasing the removal efficiency of CEX at acidic pHs is probably high concentrations of H^+ ions in acidic solutions.

Also, high removal efficiency at acidic pH can be due to the fact that at low pH, the active sites on the adsorbent surface become protonated, and the charge density on the adsorbent surface increases [44]. During the use of ultrasonic systems, when a solution is exposed to sound waves, the water vapor in the bubbles caused by the cavitation phenomenon can take the form of H^+ or OH^0, which is due to the effect pH of the environment [45–47].

The pH of the solution is an important and effective parameter in adsorption, so that it plays an important role in the entire adsorption process. The pH of the solution affects not only the surface charge of the adsorbent, but also the degree of ionization of the substance in the solution. Moreover, the separation of functional groups in the active sites of adsorbent also affects the chemistry of the solution and plays an essential role in the electrostatic attraction between the adsorbent and the adsorbate [48]. Due to the molecular structure of cefixime (CEX) and the presence of hydroxide and amine bonds, CEX tends to bond with positive charged surfaces; therefore, when the pH decreases

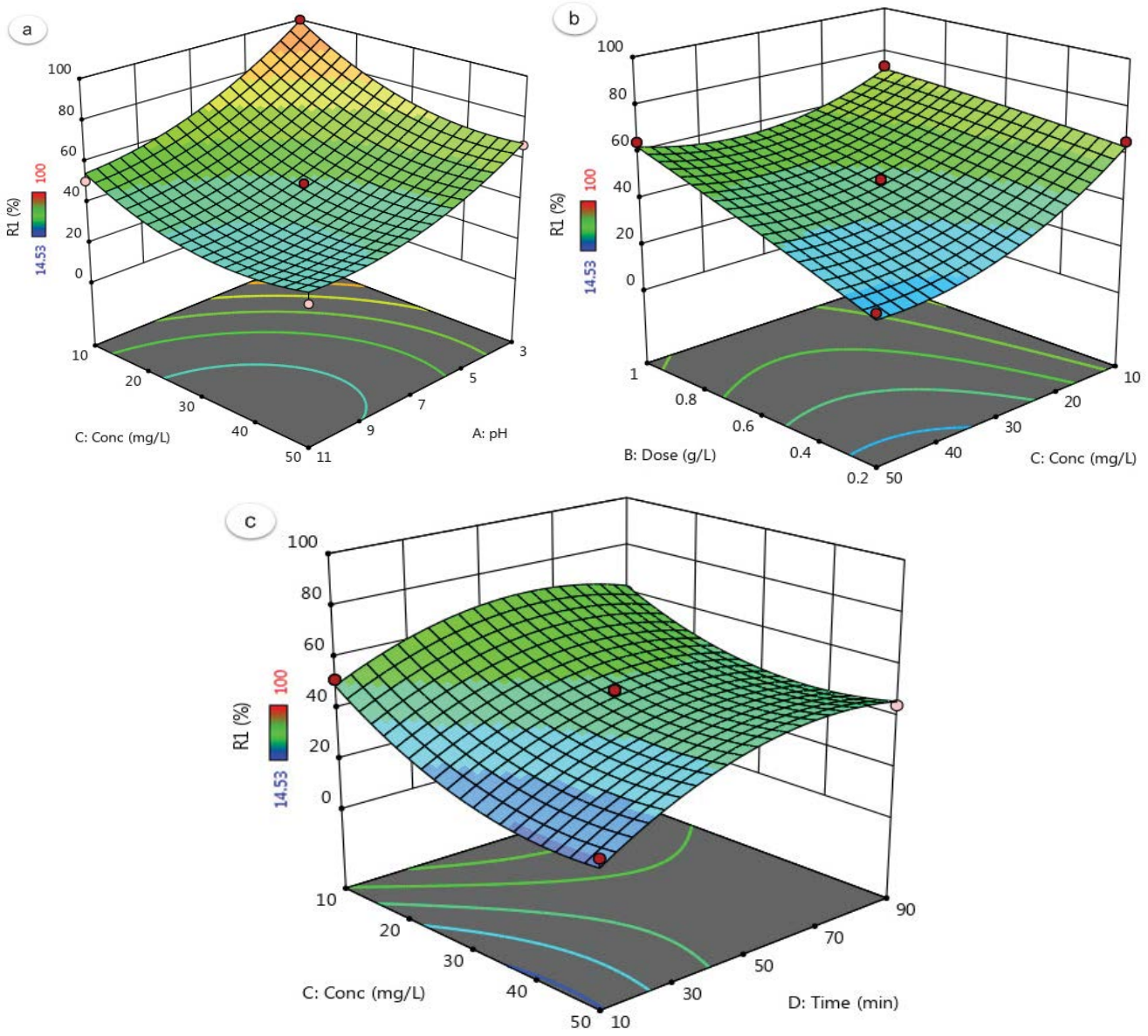

Fig. 9. CEX removal efficiency as a function of pH (a), as a function of nanocomposite concentration (b), as a function of reaction time and initial concentration of CEX (c).

due to the electrostatic attraction between the CEX and the adsorbent, the removal efficiency increases [49,50].

3.3.2. *Influence of GO-Fe_3O_4 nanocomposite dosage*

Fig. 9b shows the effect of nanocomposite concentration on the removal efficiency of CEX. Based on the obtained results, it can be said that increasing the concentration of nanoparticles up to 1 g/L has increased the efficiency. According to the analysis of this statistical model, with increasing the dose of nanoparticles, the efficiency increased, and the optimal nanoparticle concentration in the removal of the CEX was determined to be 1. The presence of GO-Fe_3O_4 nanoparticles in the sonocatalytic process provides nuclei and additional surfaces for cavitation, which in turn increases the number of bubbles and radicals in the tissue [44]. It can be attributed to the fact that when all the antibiotic molecules of CEX adsorb on the nanoparticle, the addition of higher amounts of GO-Fe_3O_4 due to the absence of antibiotic molecules had no effect on efficiency. Ultrasound generally acts as an energy source for nanoparticle activation. Nanoparticles tend to accumulate due to their high surface structure and high surface energy, but ultrasonic waves cause dispersion of these particles and lack of their accumulation. However, when the concentration of nanoparticles exceeds a certain value, the energy of the ultrasonic waves is not sufficient to scatter them, so the removal efficiency remains constant with the addition of more values [18]. The results related to the effect of nanoparticle dose in this study were similar to the results studied by Mostafa Pour and Almasi [51,52].

3.3.3. Effect of initial concentration of CEX

Fig. 9c shows the initial concentration of CEX on the removal efficiency. With increasing the initial concentration of CEX from 0.2 to 1 mg/L, the efficiency has decreased. Therefore, the optimum point for the initial concentration of CEX was determined to be 1 mg/L. Decreasing degradation rate due to increasing concentration can be attributed to competition for reaction with hydroxyl radicals at high concentrations. As the concentration increases, the partial pressure in the cavitation bubbles increases, and as a result, the bubble decomposition temperature decreases, which itself can affect the degradation of some materials. It can also be said that in sonocatalytic processes, the concentration of produced radicals is the same in all samples. Therefore, for samples with lower concentrations of the CEX and in the presence of the same amount of hydroxyl radicals, a higher rate of degradation will be obtained compared to samples with high concentrations of antibiotics [44]. Furthermore, with increasing the initial concentration of antibiotics, the number of active adsorption sites on the adsorbent surface and removal efficiency decrease. In this way, the adsorption sites on the adsorbent surface are rapidly occupied by the contaminant in the initial moments. For this reason, after that, the adsorption of pollutants takes place inside the pores and the adsorption rate also decreases [53]. This part of the results was consistent with the results of Vahidi et al. for evaluation of amoxicillin removal using zero-valent iron nanoparticles in presence of peroxide hydrogen and sonolysis process and the removal of cephalexin using activated carbon from aqueous solution [54–55].

As can be seen in Fig. 9c, as the contact time increases, the removal of CEX antibiotic increases. Also, the highest efficiency was obtained at a contact time of 90 min. The reaction time is one of the most important parameters affecting the design and performance of any chemical process. In fact, the reaction time is the time required to achieve the desired treatment goals [44]. The reason for increasing the removal efficiency in the early reaction times is to create more holes and corrosion in the nanoparticle surface and, as a result, increase the cross-sectional area of adsorption and removal efficiency [44,56]. Also, when the reaction time increases, the oxidizing agent, such as the produced hydroxyl radicals, has the opportunity to be in contact with the contaminant for a longer period of time, thus removing a higher percentage of the contaminant and increasing the removal efficiency [43]. In a study by Kamani et al. entitled the evaluation of the sononocatalytic process efficiency using titanium dioxide nanoparticles in the removal of the erythromycin and metronidazole antibiotics from aqueous media and in the study of Sobhani Kia, entitled removal of the penicillin G antibiotic from aqueous media using sing a batch reactor of zero iron nanoparticles and ozonation process, similar results have been reported for reaction time [44–57].

3.4. Determining the optimal conditions for the removal of CEX antibiotic

The main purpose of testing and optimization is to achieve the optimal values of variables for the removal of CEX from aqueous solutions. Statgraphics software version 16 was used to optimize and achieve the highest removal efficiency of CEX. The optimal conditions provided by the software are presented in Table 3. In order to validate the obtained optimal conditions, the experimental software was performed experimentally again with the optimal values provided, and the obtained result is given in Table 3. As can be seen, the experimental removal efficiency has an error of 1.79 units (about 2%) compared to the predicted efficiency, and this small difference indicates the validity of the fitted model.

3.5. Effect of ultrasonic on adsorption process at optimal condition

Sonochemical reactions caused by sonic radiation in liquids are at frequencies that produce cavitation. Therefore, cavitation acts as a means of concentrating the released energy. Ultrasound waves increase chemical and physical changes in a liquid medium by producing and destroying cavitation bubbles [58,59]. These bubbles form and grow over a period of time until they reach an equilibrium size at a certain frequency. The fate of these bubbles is to disintegrate in dense cycles to produce the energy needed for chemical and mechanical effects. In this study, ultrasonic has been used to accelerate the chemical process by creating the phenomenon of cavitation. Ultrasound, in addition to creating the cavitation phenomenon, increases the rate of material transfer in the adsorption process. The results showed that ultrasound has a promising effect on the adsorption of CEX by increasing the adsorption rate and mass transfer. As shown in Fig. 10, there is a significant difference in adsorption efficiency when ultrasonic was used at a concentration of 50 mg/L.

Ultrasound processes are one of the processes for the removal of pollutants from aqueous solution, along with other methods such as AOP. In this case, the use of ultrasonic waves for the phenomenon of acoustic cavitation, namely formation and growth, is known to accelerate chemical processes. The collapse of micrometric bubbles is formed by the propagation of pressure waves in a liquid. Ultrasound and its side effects and cavitation improve the transport of substances through the convection path resulting from physical phenomena [26].

3.6. Isotherm studies and adsorption kinetics

3.6.1. Adsorption kinetics

Kinetic equations are used to describe the transfer behavior of adsorbed material molecules per unit time or to study variables affecting the reaction rate. In the present study, pseudo-first-order and pseudo-second-order kinetic models were investigated using GO-Fe_3O_4 to investigate the factors affecting the reaction rate of the CEX adsorption process. The pseudo-first and second linear kinetic equations are expressed as Eqs. (3) and (4), respectively.

Fig. 11 shows the pseudo-first-order and pseudo-second-order kinetic models, respectively. The parameters of pseudo-first- and second-order kinetic models are shown in Table 4. According to the results obtained for CEX, the pseudo-second-order model with regression coefficient (R^2) fits better than the pseudo-first-order model with

Table 3
Optimal values of effective parameters in the process of removing CEX

System	Value
Solution pH	3
Concentration GO-Fe_3O_4, g/L	1
Initial concentration of CEX, mg/L	10
Reaction time, min	90
Predicted removal efficiency, %	100
Observed removal efficiency, %	98.21

experimental data. Asrari et al. [60], by comparing the performance of chitosan adsorbent and chitosan modified with Fe_3O_4 in erythromycin removal from water environments, reported the appropriate kinetic model for the pseudo-second-order model for the process. Also, the predicted equilibrium adsorption capacity by the pseudo-second-order kinetic model, compared to the pseudo-second-order kinetic model, has a lower difference with an experimental amount of equilibrium adsorption capacity. As presented in Table 4, the constant rate (K_2) of the pseudo-second-order has decreased with an increase in the concentration of the CEX. This tendency to decrease the speed initially is due to sufficient places in a constant level of adsorbent to adsorb lower concentrations of CEX, and the adsorption rate was higher. However, the adsorption rate of dissolved materials is also reduced gradually due to the reduction of active sites required for high concentrations of CEX.

3.6.2. Adsorption isotherms

Adsorption isotherms are adsorption properties and equilibrium data that describe how contaminants react with adsorbents and play a key role in optimizing adsorbent consumption. There are many isotherm models for analyzing experimental data and describing the equilibrium in adsorption; these models are used to provide insight into the adsorption mechanism, surface properties, and adsorption tendency and to describe the experimental adsorption data. Therefore, it is very important to make a proper connection between equilibrium diagrams to optimize the conditions and design absorption systems [61,62]. The equation of the Langmuir model is the monolayer adsorption process as follows [32]:

$$\frac{C_{eq}}{q_{eq}} = \frac{1}{Qb} + \frac{C_{eq}}{Q} \tag{3}$$

$$Rl = \frac{1}{1+bc} \tag{4}$$

where (mg/g) q_{eq} is the amount of CEX absorbed per gram of adsorbent and (mg/L) C_{eq} is the equilibrium concentration of CEX in equilibrium.

Q and b are Langmuir parameters, which are related to the maximum adsorption capacity and the adsorption correlation energy [63], respectively. One of the properties of

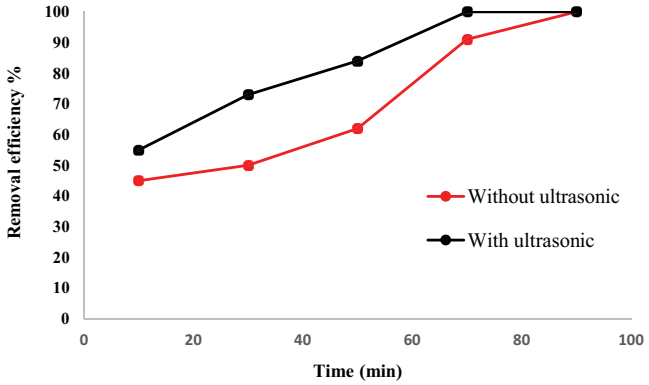

Fig. 10. Effect of ultrasonic on acceleration of process in different time in CEX concentration of 50 mg/L.

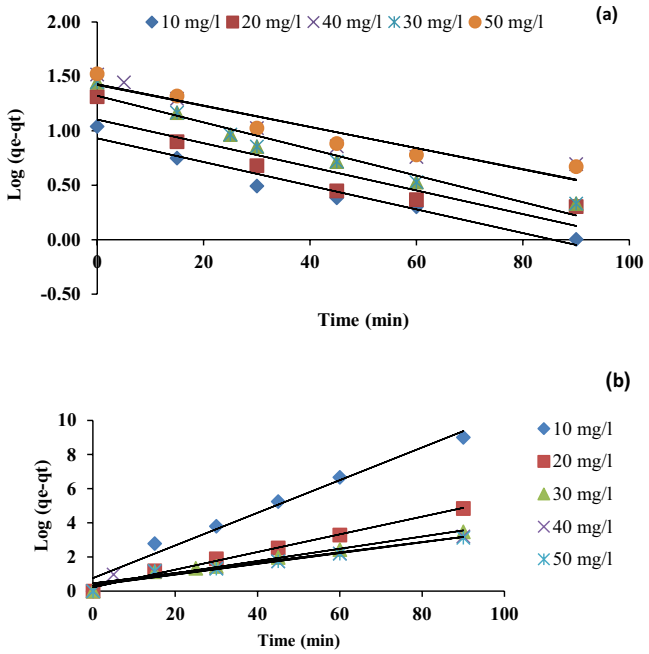

Fig. 11. Pseudo-first-order (a) and pseudo-second-order (b) kinetics model for CEX adsorption.

the Langmuir equation that can be used to determine the type of adsorption process is the dimensionless parameter of the separation coefficient R_L [Eq. (6)]. If $R_L < 1$, the type of adsorption is undesirable; if $R_L = 1$, the type of adsorption is linear; if $0 < R_L < 1$, the type of adsorption is favorable, and if $R_L = 0$, the adsorption is irreversible [64]. When the adsorption sites are uniform and the surface is uniform, the Langmuir relationship is consistent with experimental experiments. However, if the surface is heterogeneous, the Freundlich relationship, obtained by measuring the amount of adsorbed material at different pressures, provides a better description of the data. According to the Freundlich model, the adsorption process is defined by Eq. (5) [65,66]:

$$\log\left(q_e\right) = \log\left(K_f\right) + \frac{1}{n}\log\left(C_e\right) \tag{5}$$

where C_e is equilibrium concentration (mg/L), q_e is adsorption capacity at equilibrium time (mg/L), and K_f and n are Freundlich adsorption constants related to adsorption capacity and intensity [67]. In this model, n values less than one indicate poor adsorption, and values of 1–2 and 2–10 indicate moderate and desirable adsorption [68]. The values of the n and K_f coefficients were determined by the slope and intercept of the linear graph of $\log q_e$ vs. $\log C_e$, respectively. The Langmuir model diagram is more consistent with the experimental data. By comparing the correlation coefficients of these two models, it was found that the correlation coefficient of the Langmuir model (0.9972) was higher than Freundlich (0.946) (Fig. 12). As a result, the Langmuir model fits better and can well describe the dye adsorption behavior; the results indicate that the distribution of active sites on the adsorbent surface is uniform, and subsequently, the adsorption of CEX has occurred in homogeneous sites. In a study by Rahmani Sani et al. [69] entitled removal of Sulfadidiomethoxine antibiotics from aqueous solutions using model carbon nanotubes, the Langmuir model was reported to be suitable. The Langmuir and Freundlich parameters for CEX are given in Table 5. The maximum adsorption capacity for GO-Fe_3O_4 under optimal conditions in the Langmuir model was obtained to be 31.06 mg/g. There are several studies [49,50,70–73] for comparing the results of this study, which are provided in Table 6.

3.7. Regeneration of the adsorbent

The regeneration of the adsorbent is one of the most important criteria for its practical application, since some adsorbed material could be hazardous and toxic, flammable or even explosive. The CEX removal efficiency of the adsorbent has been examined after its regeneration to determine its capability to use in real wastewater treatment. The regeneration of GO/Fe_3O_4 nanocomposite was carried out by using 0.1 M HNO_3. Regenerated GO/Fe_3O_4 nanocomposites were added in 100 mg/L of pollutant solution in optimum condition, and after the equilibrium time, the regeneration of the adsorbent was investigated. These adsorption regeneration cycles were down up to five times. After the regeneration, the spent adsorbents for the next regeneration stage were dried at 100°C for 12 h. Fig. 13 shows the efficiency of regenerated adsorbent has decreased by approximately 40% in the first stage of regeneration, and the removal percentage ability after the fifth regeneration was 50%. Thus, it can be concluded from this experiment that GO/Fe_3O_4 nanocomposite has no significant capability after five consecutive cycles of regeneration for the adsorption of CEX.

Table 5
Langmuir and Freundlich isotherm coefficients

Langmuir			Freundlich		
R_L	R^2	q_m (mg/g)	R^2	n	K_f [(mg/g)(mg/L)$^{1/n}$]
0.019	0.9972	31.06	0.946	9.8	20.64

4. Conclusion

The results of this study showed that the use of RSM-BBD is a suitable method for modeling and optimizing operating parameters for CEX antibiotic removal by Fe_3O_4@

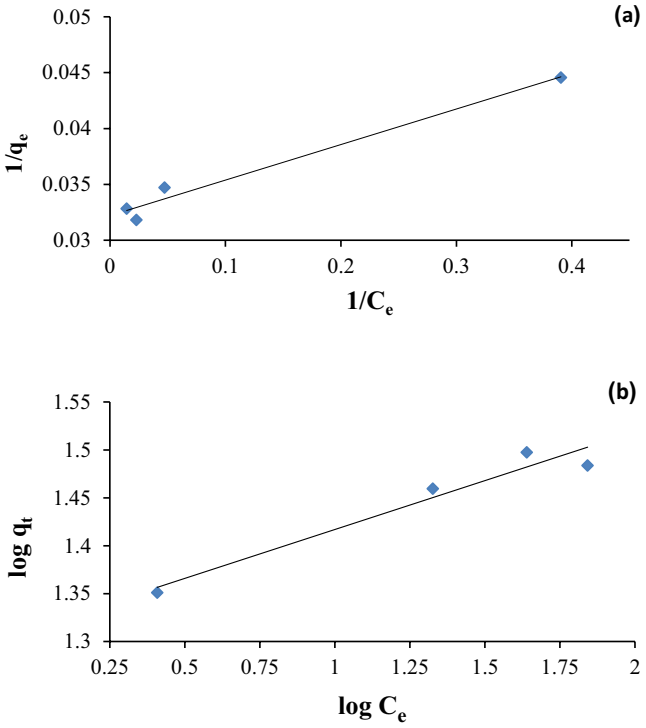

Fig. 12. Langmuir (a) and Freundlich (b) isotherms for GO-Fe_3O_4 on CEX removal efficiency.

Table 4
Calculated variables for kinetic models

Pseudo-first-order					Pseudo-second-order		
C_0 (mg/L)	$q_{e,epx}$ (mg/g)	$q_{1,cal}$ (mg/g)	k_1 (1/min)	R^2	$q_{2,cal}$ (mg/g)	k_2 (g/mg·min)	R^2
10	11	8.53	0.0251	0.9517	10.44	0.0120	0.9766
20	20.6	12.69	0.0251	0.8351	19.30	0.0122	0.9928
30	28	20.98	0.0280	0.9445	27.85	0.0039	0.9723
40	33	26.80	0.0225	0.8965	33.11	0.0020	0.9348
50	33.5	26.35	0.0221	0.9034	31.64	0.0030	0.9518

Table 6
Adsorption capacity and removal efficiency of CEX using Fe_3O_4@GO nanocomposite and other materials

Adsorbent	q_e (mg/g)	References
Magnetic nanoparticles-rGO-chitosan composite	31	[66]
Activated carbon prepared date residues	557.9 and 571.5	[43]
Modified bionanocomposite	30.5	[67]
Nano-size biomass derived from pomegranate peel	181.81	[42]
Polyelectrolyte-modified nanosilica	11	[68]
Chitosan modified nano-Al_2O_3	13	[69]
MgO NPs	526	[70]
Fe_3O_4@GO nanocomposite with ultrasonic	31	Present study

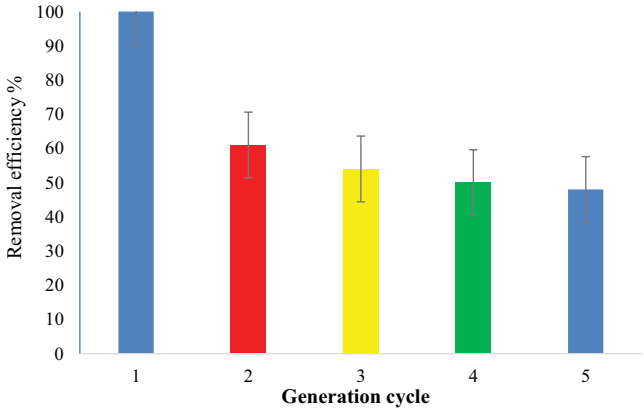

Fig. 13. CEX removal efficiency in regeneration of the adsorbent in five cycles.

GO nanocomposite process with ultrasonic. The proposed model presented by the software showed that the removal of CEX is affected by various parameters such as nanocomposite concentration, solution pH, reaction time, and initial concentration of CEX. These factors are effective in increasing the efficiency of the process due to increasing the production of hydroxyl radicals, creating a suitable adsorbent surface, and the appropriate reaction time with the contaminant. According to the results of this study, the most important parameter was pH. Results showed the adsorption process had the best efficiency at pH of 3. The optimum concentration of nanocomposite was 1 g/L; the optimal reaction time was 90 min, and the initial concentration of CEX was 10 mg/L. The highest removal rate of CEX antibiotic was obtained at 100% under optimal process conditions.

Ultrasonic, in addition to creating the cavitation phenomenon, increases the rate of material transfer in the adsorption process. The results showed that ultrasound has a promising effect on the adsorption of CEX by increasing the adsorption rate and mass transfer.

Acknowledgement

The authors of the article would like to thank the deputy of Research and Technology of Ardabil University of Medical Sciences and Health Services for financial support of this research (dissertation: No. IR.ARUMS.REC.1398.534) and the experts of the Laboratory of Environmental Chemistry and Instrumental Analysis.

Author declaration

Funding

The current study was financially supported by Ardabil University of Medical Sciences.

Conflicts of interest

The authors declare that there is no conflict of interest regarding the publication of this work.

Data availability

The dataset and analyzed during the current study are available from the corresponding authors on realistic demand.

Ethics approval and consent to participate

Not applicable

Consent for publication

Not applicable

Authorship contribution statement

Mehdi Vosoughi and Abdollah Dargahi: Conceptualization, Methodology, Validation, Formal analysis, Investigation, Resources, Supervision, Funding acquisition. Ahmad Mokhtari and Hadi Sadeghi: Methodology, Validation, Resources, Writing – original draft, Writing – review & editing. Farzad Mahdavian: Methodology, Validation, Formal analysis, Investigation, Resources, Writing – original draft. Yousef Rashtbari: Writing – original draft, Writing – review & editing, Project.

References

[1] J. Rivas, O. Gimeno, F. Beltrán, Wastewater recycling: application of ozone based treatments to secondary effluents, Chemosphere, 74 (2009) 854–859.

[2] A. Azizi, A. Dargahi, A. Almasi, Biological removal of diazinon in a moving bed biofilm reactor – process optimization with central composite design, Toxin Rev., 40 (2021) 1242–1252.
[3] M. Yilmaz, T.J. Al-Musawi, A.D. Khatibi, M. Baniasadi, D. Balarak, Synthesis of activated carbon from *Lemna minor* plant and magnetized with iron(III) oxide magnetic nanoparticles and its application in removal of ciprofloxacin, Biomass Convers. Biorefin., (2022) 1–14, doi: 10.1007/s13399-021-02279-y.
[4] M. Rakhshani, F. Rakhshani, A. Mirshahi, Self-medication in Zahedan city in 1999, 6 (2002) 45–52.
[5] T.J. Al-Musawi, A.H. Mahvi, A.D. Khatibi, D. Balarak, Effective adsorption of ciprofloxacin antibiotic using powdered activated carbon magnetized by iron(III) oxide magnetic nanoparticles, J. Porous Mater., 28 (2021) 835–852.
[6] T.J. Al-Musawi, N. Mengelizadeh, K. Sathishkumar, S. Mohebi, D. Balarak, Preparation of $CuFe_2O_4$/montmorillonite nanocomposite and explaining its performance in the sonophotocatalytic degradation process for ciprofloxacin, Colloid Interface Sci. Commun., 45 (2021) 100532, doi: 10.1016/j.colcom.2021.100532.
[7] M. Heidari, M. Vosoughi, H. Sadeghi, A. Dargahi, S.A. Mokhtari, Degradation of diazinon from aqueous solutions by electro-Fenton process: effect of operating parameters, intermediate identification, degradation pathway, and optimization using response surface methodology (RSM), Sep. Sci. Technol., 56 (2021) 2287–2299.
[8] T.J. Al-Musawi, P. Rajiv, N. Mengelizadeh, F.S. Arghavan, D. Balarak, Photocatalytic efficiency of $CuNiFe_2O_4$ nanoparticles loaded on multi-walled carbon nanotubes as a novel photocatalyst for ampicillin degradation, J. Mol. Liq., 337 (2021) 116470, doi: 10.1016/j.molliq.2021.116470.
[9] W.-h. Xu, G. Zhang, S.-c. Zou, X.-d. Li, Y.-c. Liu, Determination of selected antibiotics in the Victoria Harbour and the Pearl River, South China using high-performance liquid chromatography-electrospray ionization tandem mass spectrometry, Environ. Pollut., 145 (2007) 672–679.
[10] G.A. Rumman, T.J. Al-Musawi, M. Sillanpaa, D. Balarak, Adsorption performance of an amine-functionalized MCM–41 mesoporous silica nanoparticle system for ciprofloxacin removal, Environ. Nanotechnol. Monit. Manage., 16 (2021) 100536, doi: 10.1016/j.enmm.2021.100536.
[11] H. Liu, W. Liu, J. Zhang, C. Zhang, L. Ren, Y. Li, Removal of cephalexin from aqueous solutions by original and Cu(II)/Fe(III) impregnated activated carbons developed from lotus stalks: kinetics and equilibrium studies, J. Hazard. Mater., 185 (2011) 1528–1535.
[12] S. Zheng, C. Cui, Q. Liang, X. Xia, F. Yang, Ozonation performance of WWTP secondary effluent of antibiotic manufacturing wastewater, Chemosphere, 81 (2010) 1159–1163.
[13] N. Olfatmehr, B. Kakavandi, S.M. Khezri, Peroxydisulfate activation by enhanced catalytic activity of $CoFe_2O_4$ anchored on activated carbon: a new sulfate radical-based oxidation study on the cefixime degradation, Sep. Purif. Technol., 302 (2022) 121991, doi: 10.1016/j.seppur.2022.121991.
[14] Z. Ciğeroğlu, Preparation of ZnO/$BaTiO_3$ adsorbent using *Elaeagnus angustifolia* L. leaf extract and its evaluation for ciprofloxacin removal from aqueous solutions: an optimization study, Biomass Convers. Biorefin., 11 (2021) 1407–1417.
[15] A. Almasi, A. Dargahi, M. Mohammadi, A. Azizi, A. Karami, F. Baniamerian, Application of response surface methodology on cefixime removal from aqueous solution by ultrasonic/photooxidation, Int. J. Pharm. Technol., 8 (2016) 16728–16736.
[16] D. Rawat, A.S. Hasan, M.R. Capoor, S. Sarma, D. Nair, M. Deb, P. Pillai, P. Aggarwal, In vitro evaluation of a new cefixime-clavulanic acid combination for gram-negative bacteria, Southeast Asian J. Trop. Med. Public Health, 40 (2009) 131–139.
[17] L. Lloret, G. Eibes, T. Lú-Chau, M.T. Moreira, G. Feijoo, J.M. Lema, Laccase-catalyzed degradation of anti-inflammatories and estrogens, BioChem. Eng. J., 51 (2010) 124–131.
[18] M. Hoseini, G.H. Safari, H. Kamani, J. Jaafari, A. Mahvi, Survey on removal of tetracycline antibiotic from aqueous solutions by nano-sonochemical process and evaluation of the influencing parameters, Iran. J. Health Environ., 8 (2015).
[19] M. Zazouli, M. Ulbricht, S. Naseri, H. Susanto, Effect of hydrophilic and hydrophobic organic matter on amoxicillin and cephalexin residuals rejection from water by nanofiltration, J. Environ. Health Sci. Eng., 7 (2010) 15–24.
[20] M. Yegane Badi, A. Esrafili, H. Pasalari, S. Fallah Jokandan, M. Farzadkia, Evaluation the efficiency of catalytic ozonation by magnetic nanoparticles TiO_2/Fe_3O_4 in removal of ceftazide antibiotic from aqueous solutions, J. Environ. Health Eng., 7 (2020) 119–134.
[21] A. Amouei, D. Naghipour, K. Taghavi, M. Estaji, Removal of metronidazole antibiotic from hospital wastewater by biosorbent prepared from plantain wood, J. Babol Univ. Med. Sci., 22 (2020) 45–52.
[22] B. Kakavandi, R. Rezaei Kalantary, A. Jonidi Jafari, A. Esrafily, A. Gholizadeh, A. Azari, Efficiency of powder activated carbon magnetized by Fe_3O_4 nanoparticles for amoxicillin removal from aqueous solutions: equilibrium and kinetic studies of adsorption process, Iran. J. Health Environ., 7 (2014) 21–34.
[23] S. Esplugas, D.M. Bila, L.G.T. Krause, M. Dezotti, Ozonation and advanced oxidation technologies to remove endocrine disrupting chemicals (EDCs) and pharmaceuticals and personal care products (PPCPs) in water effluents, J. Hazard. Mater., 149 (2007) 631–642.
[24] S. Shen, J. Ren, J. Chen, X. Lu, C. Deng, X. Jiang, Development of magnetic multi-walled carbon nanotubes combined with near-infrared radiation-assisted desorption for the determination of tissue distribution of doxorubicin liposome injects in rats, J. Chromatogr. A, 1218 (2011) 4619–4626.
[25] M. Iram, C. Guo, Y. Guan, A. Ishfaq, H. Liu, Adsorption and magnetic removal of neutral red dye from aqueous solution using Fe_3O_4 hollow nanospheres, J. Hazard. Mater., 181 (2010) 1039–1050.
[26] S. Dashamiri, M. Ghaedi, K. Dashtian, M.R. Rahimi, A. Goudarzi, R. Jannesar, Ultrasonic enhancement of the simultaneous removal of quaternary toxic organic dyes by CuO nanoparticles loaded on activated carbon: central composite design, kinetic and isotherm study, Ultrason. Sonochem., 31 (2016) 546–557.
[27] M.D. Tezerjani, A. Benvidi, A.D. Firouzabadi, M. Mazloum-Ardakani, A. Akbari, Epinephrine electrochemical sensor based on a carbon paste electrode modified with hydroquinone derivative and graphene oxide nano-sheets: simultaneous determination of epinephrine, acetaminophen and dopamine, Measurement, 101 (2017) 183–189.
[28] C. Santhosh, E. Daneshvar, P. Kollu, S. Peräniemi, A.N. Grace, A. Bhatnagar, Magnetic SiO_2@$CoFe_2O_4$ nanoparticles decorated on graphene oxide as efficient adsorbents for the removal of anionic pollutants from water, Chem. Eng. J., 322 (2017) 472–487.
[29] A. Amouei, H. Asgharnia, K. Karimian, Y. Mahdavi, D. Balarak, S. Ghasemi, Optimization of dye reactive orange 16 (RO16) adsorption by modified sunflower stem using response surface method from aqueous solutions, J. Rafsanjan Univ. Med. Sci., 14 (2016) 813–826.
[30] M. Ghorbani, A. Bagherian, Optimization of astrazon blue adsorption onto sulfunated styrene-co-divinylbenzene resin by experimental design methodology, Nashrieh Shimi va Mohandesi Shimi Iran, 35 (2016) 25–37.
[31] L. Järup, Hazards of heavy metal contamination, Br. Med. Bull., 68 (2003) 167–182.
[32] A. Dargahi, M.R. Samarghandi, A. Shabanloo, M.M. Mahmoudi, H.Z. Nasab, Statistical modeling of phenolic compounds adsorption onto low-cost adsorbent prepared from aloe vera leaves wastes using CCD-RSM optimization: effect of parameters, isotherm, and kinetic studies, Biomass Convers. Biorefin., (2021) 1–15, doi: 10.1007/s13399-021-01601-y.
[33] A. Dargahi, M. Vosoughi, S.A. Mokhtari, Y. Vaziri, M. Alighadri, Electrochemical degradation of 2,4-dinitrotoluene (DNT) from aqueous solutions using three-dimensional electrocatalytic reactor (3DER): degradation pathway, evaluation of toxicity and optimization using RSM-CCD, Arabian J. Chem., 15 (2022) 103648, doi: 10.1016/j.arabjc.2021.103648.
[34] M.R. Samarghandi, A. Dargahi, A. Rahmani, A. Shabanloo, A. Ansari, D. Nematollahi, Application of a fluidized three-dimensional electrochemical reactor with Ti/SnO_2–Sb/β-PbO_2

anode and granular activated carbon particles for degradation and mineralization of 2,4-dichlorophenol: process optimization and degradation pathway, Chemosphere, 279 (2021) 130640, doi: 10.1016/j.chemosphere.2021.130640.
[35] H.V. Tran, L.T. Bui, T.T. Dinh, D.H. Le, C.D. Huynh, A.X. Trinh, Graphene oxide/Fe_3O_4/chitosan nanocomposite: a recoverable and recyclable adsorbent for organic dyes removal. Application to methylene blue, Mater. Res. Express, 4 (2017) 035701, doi: 10.1088/2053-1591/aa6096.
[36] Y. Jiang, J.-L. Gong, G.-M. Zeng, X.-M. Ou, Y.-N. Chang, C.-H. Deng, J. Zhang, H.-Y. Liu, S.-Y. Huang, Magnetic chitosan–graphene oxide composite for anti-microbial and dye removal applications, Int. J. Biol. Macromol., 82 (2016) 702–710.
[37] K. Hasani, A. Peyghami, A. Moharrami, M. Vosoughi, A. Dargahi, The efficacy of sono-electro-Fenton process for removal of cefixime antibiotic from aqueous solutions by response surface methodology (RSM) and evaluation of toxicity of effluent by microorganisms, Arabian J. Chem., 13 (2020) 6122–6139.
[38] S. Afshin, Y. Rashtbari, M. Vosough, A. Dargahi, M. Fazlzadeh, A. Behzad, M. Yousefi, Application of Box–Behnken design for optimizing parameters of hexavalent chromium removal from aqueous solutions using Fe_3O_4 loaded on activated carbon prepared from alga: kinetics and equilibrium study, J. Water Process. Eng., 42 (2021) 102113, doi: 10.1016/j.jwpe.2021.102113.
[39] A. Dargahi, K. Hasani, S.A. Mokhtari, M. Vosoughi, M. Moradi, Y. Vaziri, Highly effective degradation of 2,4-dichlorophenoxyacetic acid herbicide in a three-dimensional sono-electro-Fenton (3D/SEF) system using powder activated carbon (PAC)/Fe_3O_4 as magnetic particle electrode, J. Environ. Chem. Eng., 9 (2021) 105889, doi: 10.1016/j.jece.2021.105889.
[40] V. Ganesan, C. Louis, S.P. Damodaran, Graphene oxide-wrapped magnetite nanoclusters: a recyclable functional hybrid for fast and highly efficient removal of organic dyes from wastewater, J. Environ. Chem. Eng., 6 (2018) 2176–2190.
[41] Y. Yao, S. Miao, S. Liu, L.P. Ma, H. Sun, S. Wang, Synthesis, characterization, and adsorption properties of magnetic Fe_3O_4@ graphene nanocomposite, Chem. Eng. J., 184 (2012) 326–332.
[42] H. Kamani, E. Bazrafshan, S.D. Ashrafi, F. Sancholi, Efficiency of sono-nano-catalytic process of TiO_2 nano-particle in removal of erythromycin and metronidazole from aqueous solution, J. Maz. Univ. Med. Sci., 27 (2017) 140–154.
[43] H.R. Sobhi, B.M. Yegane, A. Esrafili, M. Ghambarian, Evaluation of the efficiency of a photocatalytic process using the magnetic nanocatalyst (Fe_3O_4@SiO_2@TiO_2) in the removal of ceftriaxone from aqueous solutions, J. Environ. Health Eng., 7 (2020) 229–243.
[44] H. Hemmati, E. Bazrafshan, H. Kamani, J. Mosafer, D. Balarak, F. Kord Mostafapour, Optimization of sono-nanocatalytic process using γ-Fe_2O_3 for penicilin antibiotic removal by response surface methodology, J. Torbat Heydariyeh Univ. Med. Sci., 5 (2017) 1–16.
[45] H. Kamani, A. Hossein Panahi, E. Norabadi, Gh. Abi, Performance evaluation of combined ultrasonic-persulfate processes in organic matter reduction of synthetic dairy wastewater, J. Birjand Univ. Med. Sci., 26 (2019) 32–43.
[46] A. Seid-Mohammadi, G. Asgarai, Z. Ghorbanian, A. Dargahi, The removal of cephalexin antibiotic in aqueous solutions by ultrasonic waves/hydrogen peroxide/nickel oxide nanoparticles (US/H_2O_2/NiO) hybrid process, Sep. Sci. Technol., 55 (2020) 1558–1568.
[47] A. Dargahi, H. Rahimzadeh Barzoki, M. Vosoughi, S.A. Mokhtari, Enhanced electrocatalytic degradation of 2,4-dinitrophenol (2,4-DNP) in three-dimensional sono-electrochemical (3D/SEC) process equipped with Fe/SBA-15 nanocomposite particle electrodes: degradation pathway and application for real wastewater, Arabian J. Chem., 15 (2022) 103801, doi: 10.1016/j.arabjc.2022.103801.
[48] R. Guo, J. Chen, Application of alga-activated sludge combined system (AASCS) as a novel treatment to remove cephalosporins, Chem. Eng. J., 260 (2015) 550–556.
[49] M. Esmaeili Bidhendi, Z. Poursorkh, H. Sereshti, H. Rashidi Nodeh, S. Rezania, M. Afzal Kamboh, Nano-size biomass derived from pomegranate peel for enhanced removal of cefixime antibiotic from aqueous media: kinetic, equilibrium and thermodynamic study, Int. J. Environ. Res. Public Health, 17 (2020) 4223, doi: 10.3390/ijerph17124223.
[50] V. Hasanzadeh, O. Rahmanian, M. Heidari, Cefixime adsorption onto activated carbon prepared by dry thermochemical activation of date fruit residues, Microchem. J., 152 (2020) 104261, doi: 10.1016/j.microc.2019.104261.
[51] F. KordMostafapour, E. Bazrafshan, D. Belarak, N. Khoshnamvand, Survey of photo-catalytic degradation of ciprofloxacin antibiotic using copper oxide nanoparticles (UV/CuO) in aqueous environment, J. Rafsanjan Univ. Med. Sci., 15 (2016) 307–318.
[52] F. Almasi, E. Dehghanifard, E. Mohammadi Kalhori, Application of photocatalytic process using Fe_3O_4/TiO_2 nanocomposite coreshell on the removal of cefixim antibiotic from aqueous solutions, J. Environ. Health Eng., 7 (2020) 384–400.
[53] M. Mohammadi Amini, M. Nourisepehr, E. Dehghanifard, Evaluation the efficiency of magnetic-metallic chitosan nanocomposite adsorbent in the removal of tetracycline antibiotic from aqueous solutions, J. Environ. Health Eng., 6 (2019) 356–374.
[54] H. Vahidi, S. Rahmani, Amoxicillin removal from aqueous solutions using US/H_2O_2/NZVI process, J. Environ. Health Eng., 5 (2018) 184–196.
[55] M. Hemmati, A. Ghaemi, H. Tavakkoli, Removal of cephalexin from aqueous solutions by activated carbon adsorbent, J. Res. Environ. Health, 5 (2019) 11–20.
[56] R. Zangi, Performance evaluation of advanced oxidation process US/UV/H_2O_2 on removal of tetracycline antibiotic from aqueous solutions, J. Sabzevar Univ. Med. Sci., 25 (2018) 143–149.
[57] M. Sobhanikia, E. Bazrafshan, H. Kamani, Removal of penicillin g from aqueous environments by batch reactor nanoparticles zero valent iron and ozonation process, J. Sabzevar Univ. Med. Sci., 24 (2017) 144–137.
[58] S. Khanjani, A. Morsali, Ultrasound-promoted coating of MOF-5 on silk fiber and study of adsorptive removal and recovery of hazardous anionic dye "Congo red", Ultrason. Sonochem., 21 (2014) 1424–1429.
[59] M. Jamshidi, M. Ghaedi, K. Dashtian, S. Hajati, A. Bazrafshan, Ultrasound-assisted removal of Al^{3+} ions and Alizarin red S by activated carbon engrafted with Ag nanoparticles: central composite design and genetic algorithm optimization, RSC Adv., 5 (2015) 59522–59532.
[60] M. Ghodrat, E. Asrari, Comparative study of the performance of chitosan and chitosan adsorbents modified with Fe_3O_4 to eliminate erythromycin from aqueous solutions, Iran. J. Health Environ., 10 (2018) 471–482.
[61] S.-L. Hii, S.-Y. Yong, C.-L. Wong, Removal of rhodamine B from aqueous solution by sorption on *Turbinaria conoides* (Phaeophyta), J. Appl. Phycol., 21 (2009) 625–631.
[62] A.H. Mahvi, M. Vosoughi, M.J. Mohammadi, A. Asadi, B. Hashemzadeh, A. Zahedi, S. Pourfadakar, Sodium dodecyl sulfate modified-zeolite as a promising adsorbent for the removal of natural organic matter from aqueous environments, Health Scope, 5 (2016) e29966, doi: 10.17795/jhealthscope-29966.
[63] H. Biglari, S. RodríguezíCouto, Y.O. Khaniabadi, H. Nourmoradi, M. Khoshgoftar, A. Amrane, M. Vosoughi, S. Esmaeili, R. Heydari, M.J. Mohammadi, Cationic surfactant-modified clay as an adsorbent for the removal of synthetic dyes from aqueous solutions, Int. J. Chem. React. Eng., 16 (2018) 1–26.
[64] A.H. Mahvi, B. Heibati, Removal efficiency of azo dyes from textile effluent using activated carbon made from walnut wood and determination of isotherms of Acid red 18, J. Health, 1 (2010) 7–15.
[65] A. Peyghami, A. Moharrami, Y. Rashtbari, S. Afshin, M. Vosuoghi, A. Dargahi, Evaluation of the efficiency of magnetized clinoptilolite zeolite with Fe_3O_4 nanoparticles on the removal of Basic violet 16 (BV16) dye from aqueous solutions, J. Dispersion Sci. Technol., (2021) 1–10, doi: 10.1080/01932691.2021.1947847.

[66] T.J. Al-Musawi, N. Mengelizadeh, M. Taghavi, S. Mohebi, D. Balarak, Activated carbon derived from *Azolla filiculoides* fern: a high-adsorption-capacity adsorbent for residual ampicillin in pharmaceutical wastewater, Biomass Convers. Biorefin., (2021) 1–13, doi: 10.1007/s13399-021-01962-4.
[67] M.V. Niri, A.H. Mahvi, M. Alimohammadi, M. Shirmardi, H. Golastanifar, M.J. Mohammadi, A. Naeimabadi, M. Khishdost, Removal of natural organic matter (NOM) from an aqueous solution by NaCl and surfactant-modified clinoptilolite, J. Water Health, 13 (2015) 394–405.
[68] Y.-M. Hao, C. Man, Z.-B. Hu, Effective removal of Cu(II) ions from aqueous solution by amino-functionalized magnetic nanoparticles, J. Hazard. Mater., 184 (2010) 392–399.
[69] A.R. Sani, A. Hosseini-Bandehgharaei, M. Naeemi, A. Navidzadeh, E. Agheli, Removal of sulfadimethoxine antibiotic from aqueous solutions using carbon nanotubes, Int. J. Environ. Health Res., 4 (2018) 11–20.
[70] Z. Ciğeroğlu, G. Küçükyıldız, B. Erim, E. Alp, Easy preparation of magnetic nanoparticles-rGO-chitosan composite beads: optimization study on cefixime removal based on RSM and ANN by using genetic algorithm approach, J. Mol. Struct., 1224 (2021) 129182, doi: 10.1016/j.molstruc.2020.129182.
[71] S. Zavareh, T. Eghbalazar, Efficient and selective removal of cefixime form aqueous solution by a modified bionanocomposite, J. Environ. Chem. Eng., 5 (2017) 3337–3347.
[72] T.H. Dao, T.T. Tran, V.R. Nguyen, T.N.M. Pham, C.M. Vu, T.D. Pham, Removal of antibiotic from aqueous solution using synthesized TiO_2 nanoparticles: characteristics and mechanisms, Environ. Earth Sci., 77 (2018) 1–14.
[73] A. Fakhri, S. Adami, Adsorption and thermodynamic study of Cephalosporins antibiotics from aqueous solution onto MgO nanoparticles, J. Taiwan Inst. Chem. Eng., 45 (2014) 1001–1006.